Energy-momentum density of graphite by $(e,2e)$ spectroscopy

M. Vos, Z. Fang, S. Canney, A. Kheifets, and I. E. McCarthy
Electronic Structure of Materials Centre, Flinders University of South Australia, GPO Box 2100, Adelaide 5001, Australia

E. Weigold
Institute of Advanced Studies, the Australian National University, Canberra 0200, Australia
(Received 10 March 1997)

The energy-resolved electron momentum density of graphite has been measured along a series of well-defined directions using $(e,2e)$ spectroscopy. This is the first measurement of this kind, to our knowledge, performed on a single-crystal target with a thoroughly controlled orientation which clearly demonstrates the different nature of the σ and π bands in graphite. Good agreement between the calculated density and the measured one is found, further establishing the fact that $(e,2e)$ spectroscopy yields more direct and complete information on the valence electronic structure than any other method. [S0163-1829(97)04627-4]

A large number of important physical properties of materials can be derived from one's knowledge of the electron wave function. Therefore a major aim of physics is to obtain the most direct information about the wave function of electrons in atoms, molecules, and solids. $(e,2e)$ spectroscopy, also called electron-momentum spectroscopy (EMS), claims to do so for occupied states. In the independent-particle approximation these measurements can be interpreted in terms of the magnitudes of the momentum space energy-resolved orbitals.

In a crystal we can write the electron wave function, in terms of Bloch functions:

$$\psi_{j\mathbf{k}}(\mathbf{r}) = \sum_{\mathbf{G}} c_{\mathbf{G}}^{j\mathbf{k}} e^{i\mathbf{G}\cdot\mathbf{r}} e^{i\mathbf{k}\cdot\mathbf{r}}, \tag{1}$$

where $\mathbf{k}$ is the crystal momentum, $\mathbf{G}$ the reciprocal lattice vector. For each $\mathbf{k}$ value there are different Bloch functions, labeled by a band index j with generally different energies $E_{j\mathbf{k}}$. For the first band the largest value of $|c_{\mathbf{G}}^{j\mathbf{k}}|$ will be for $\mathbf{k}+\mathbf{G}$ in the first Brillouin zone (BZ), for the second band for $\mathbf{k}+\mathbf{G}$ in the second BZ, etc. The momentum space representation of $\psi_{j\mathbf{k}}(\mathbf{r})$ is simply given by

$$\phi_{j\mathbf{k}}(\mathbf{q}) = \sum_{\mathbf{G}} c_{\mathbf{G}}^{j\mathbf{k}} \delta_{\mathbf{k}+\mathbf{G},\mathbf{q}}. \tag{2}$$

In these $(e,2e)$ experiments a well-collimated beam of energetic electrons ($\simeq 20.8$ keV in the present study) impinges on an extremely thin ($\leqslant 150$ Å) target. A fraction of the incoming electrons transfers a large amount of energy to a target electron in a binary collision. If one determines the energy and the momentum of the scattered and ejected electrons *in coincidence* one can infer the binding energy ε and momentum $\boldsymbol{q}$ of the target electron *before* the collision from the conservation laws. The intensity measured in an ideal $(e,2e)$ experiment (without multiple scattering) is proportional to the energy-resolved electron momentum density

$$\rho(\varepsilon,\boldsymbol{q}) = \sum_{j,\mathbf{G}} |c_{\mathbf{G}}^{j\mathbf{k}}|^2 \delta(\varepsilon - E_{j\mathbf{k}})\, \delta_{\mathbf{k}+\mathbf{G},\mathbf{q}}. \tag{3}$$

It is the most complete description of the electron distribution in solids available. More generally, in a real solid, where correlation effects may be important, the independent-particle orbital in Eqs. (1)–(3) has to be replaced by the quasiparticle orbital and the $(e,2e)$ cross section becomes sensitive to correlation effects.[1] This spectroscopy has been successfully applied to atoms and molecules,[1] and to a more limited extent to solids.[2,3]

Other techniques measure quantities derived from the energy-momentum density. In particular, $(\gamma,e\gamma)$ spectroscopy measures the (energy-integrated) momentum density.[4] In Compton scattering experiments the momentum density is integrated over energy but in addition, one measures only the projection of the momentum along the scattering vector (see, e.g., Ref. 5). On the other hand, photoemission experiments measure for single crystals (if one avoids problems with refraction of electrons at the surface) the energy difference between different states with equal crystal momentum, from which the energy-momentum density itself cannot be inferred. In other words, photoemission determines (with great accuracy) the energy-dispersion relation between ε and $\mathbf{k}$, but cannot provide a direct experimental estimate of the magnitude of the momentum space representation of the wave function, even for a crystal. In photoemission one can calculate approximately the expected photoelectron intensity from a model of the initial and final state wave function. For graphite this was done recently by Nishimoto *et al.*[6] who found qualitative agreement between the measured intensity of the π band and the intensity calculated using a tight binding model. As well as being able to measure energy-momentum dispersion in ordered as well as disordered materials we want to show here that EMS reveals other important physical properties, specifically the energy-resolved magnitude of the wave function in momentum representation.

There are two main reasons why $(e,2e)$ spectroscopy, despite its enormous potential, has not been a widely used

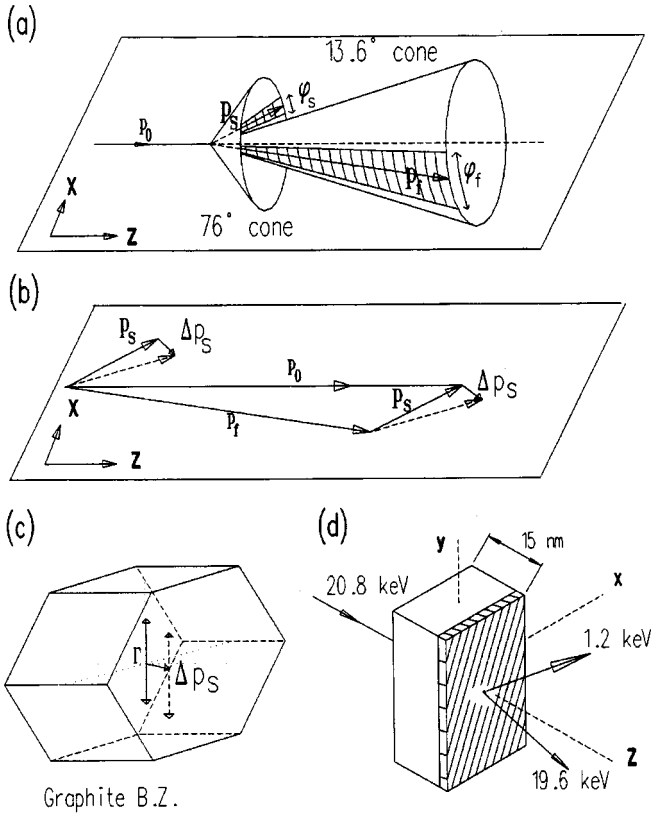

FIG. 1. In (a) we show the range of angles (i.e., momenta) measured simultaneously by our analyzers of the fast (f) and slow (s) electrons. In (b) we show that for the standard position of the slow analyzer, if all three vectors are in the same plane, $\boldsymbol{p}_o=\boldsymbol{p}_s+\boldsymbol{p}_f$, i.e., coincidences under these conditions correspond to $\boldsymbol{q}=\mathbf{0}$ (solid arrows). If all three electrons are not in the same plane the corresponding $\mathbf{q}$ vector would be directed approximately along the y axis. Rotation of the slow electron detector introduces a small additional vector $\Delta\boldsymbol{k}_s$, oriented in the x-z plane (dotted arrows). In (c) we show that in the standard position the range of $\mathbf{q}$ values we can access is along a line through Γ. After the rotation of the slow electron analyzer this line has shifted away from Γ by $\Delta\boldsymbol{k}_s$. In (d) we show the thin film and the incoming and outgoing trajectories. Due to the small mean free path of the slow electron most information is obtained from the hatched part of the crystal.

spectroscopic tool. In the first place it is a coincidence technique, and therefore the data accumulation is very slow. The first measurements of the valence band of solids had poor statistics and limited energy and momentum resolution.[7,8] These problems were overcome to a great extent by the use of two-dimensional detectors[9] and the use of a monochromatized electron beam.[10] With these improvements we can measure the energy-momentum density along a certain momentum direction in about two days with an energy resolution of 0.9 eV and a momentum resolution of 0.10 a.u. (Here and throughout we use the atomic units of momentum 1 a.u. $= 1.89\ \text{Å}^{-1}$ by setting $\hbar = 1$, and thereby equating momenta and wave numbers.) Our results extend the low resolution and poor statistics measurements of Gao *et al.*,[8] and make a much more complete comparison between experiment and theory feasible.

The second problem is the multiple scattering, both elastic and inelastic, suffered by the incident and outgoing electrons. If multiple scattering occurs we infer from the conservation laws the wrong values of ε or $\mathbf{q}$. Even for the extremely thin films used here ($\simeq$ 150 Å) it causes $\rho(\varepsilon,\boldsymbol{q})$ to be superimposed on a smooth background. At these high kinetic energies the transport of electrons in solids is quite well understood and multiple-scattering effects can be readily modeled.[11]

The experimental setup used in the present study is illustrated in Fig. 1. In order to reduce the data acquisition time we use two electron analyzers that both measure simultaneously a range of energies and momenta. By choosing the incoming and outgoing energies carefully, in combination with the appropriate scattering angles of the slow and fast electrons, we can ensure that if the incident and outgoing electrons are all in the same plane then $\boldsymbol{p}_o=\boldsymbol{p}_s+\boldsymbol{p}_f$, i.e., the target electron momentum $\boldsymbol{q}=\mathbf{0}$. Here labels o, s, f indicate the incident and the slow and the fast outgoing electrons, respectively. If the electrons are not all in the same plane then $\boldsymbol{q}$ is directed approximately along the vertical direction (also chosen as the y direction). This detector position is referred to as the standard position. By moving the slow electron detector forward or backward we can measure electrons with $\boldsymbol{q}$ vectors that have components perpendicular to the vertical direction. As a check of the geometry we ascertain that if we move the slow electron detector forward or backward by the same amount we measure a distribution that varies symmetrically around this standard position.

The thin single-crystal films were prepared from natural graphite (from Ticonderoga, NY) by cleaving and then further thinning by exposure to a low-energy Ar/O_2 plasma beam.[12] The final free-standing membrane was annealed to desorb any adsorbed oxygen. The sample could be rotated around the direction normal to the (horizontal) surface. In this way we can choose the orientation of the line along which we measure the momentum densities relative to the crystal axes. This orientation was determined by transmission electron diffraction. $(e,2e)$ measurements were made with the crystal oriented in such a way that either the Γ-K or the Γ-M directions were made vertical (i.e., along the y direction). Unfortunately we could only get to within 5° of the Γ-M direction, due to mechanical constraints. In the remainder of this paper we shall refer to this orientation simply as Γ-M, but the calculations were carried out including this 5° offset.

In total we measured spectra along 20 different lines in momentum space. Each measurement took 2–4 days. There was no sign of deterioration of the crystal during all of these measurements. Some of our results are shown as gray-scale plots in Fig. 2. Here we present measurements along (a) the Γ-M direction, (b) the Γ-K direction, and (c) along a line parallel to the Γ-K direction, but displaced by 0.55 a.u. along the Γ-M direction and 0.41 a.u. along the c axis (Γ-A direction, also chosen as the z direction). The total momentum range over which information is obtained extends from approximately -3 a.u. to 3 a.u. The energy is expressed relative to the vacuum level, the natural reference point in this type of experiment. The separation of the vacuum level and the Fermi level for this spectrometer is not clearly evident in the graphite spectra as it is a semimetal. From other measurements this separation is known to be at 5 ± 0.5 eV.

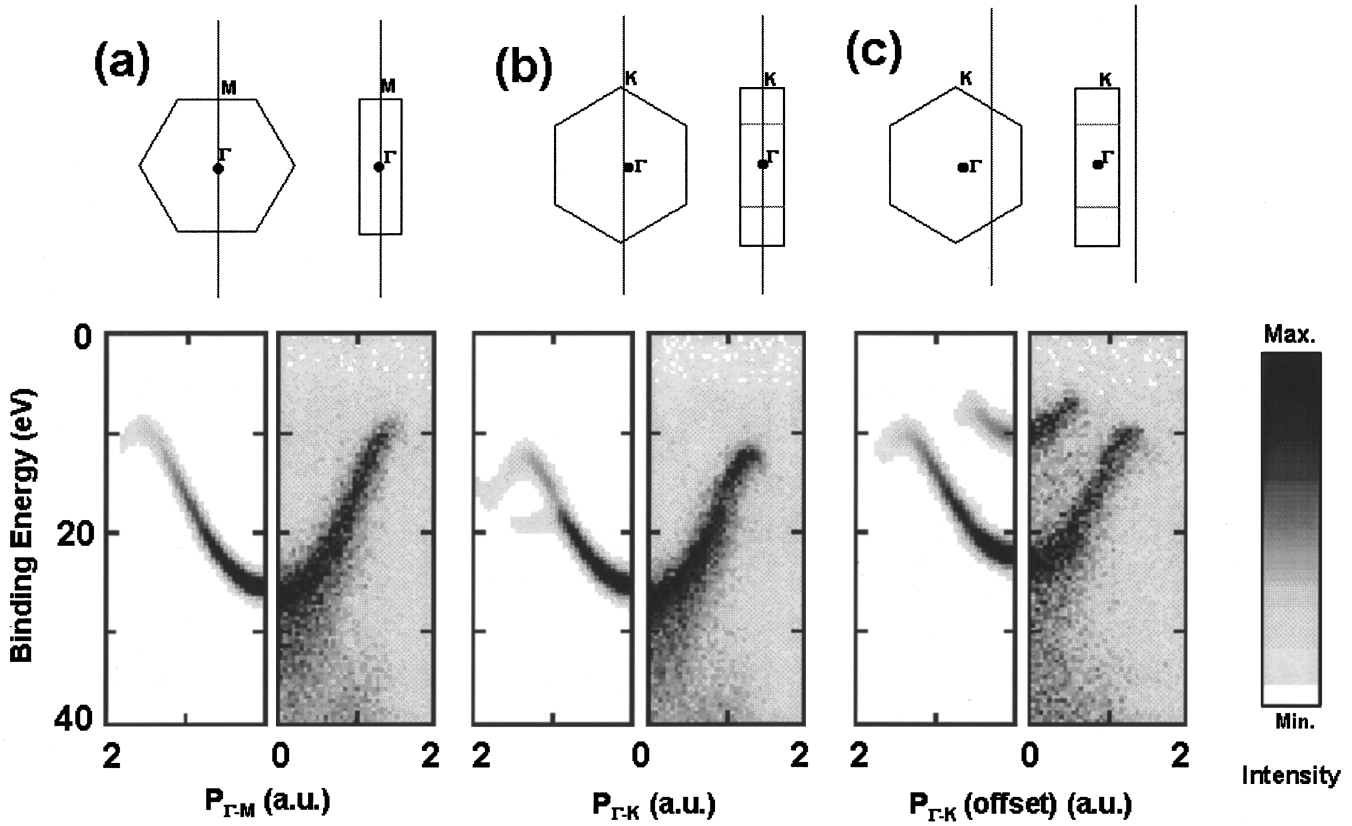

FIG. 2. The measured intensity as a function of binding energy and momentum q_y for three different measurement geometries. Also shown are the results of LMTO calculations convoluted with 2 eV energy resolution and a momentum resolution of 0.1 a.u. The momentum space directions are indicated on the Brillouin zone schemes in two projections to highlight both the q_{xy}, and q_{xz} momentum components.

A qualitative analysis of the experimental results can be performed using theoretical electron momentum densities of graphite calculated along several high symmetry directions by Kheifets and Vos.[13] In general, graphite has four populated bands, three σ and one π. However, the number of bands populated, can be reduced due to the symmetry in some directions. For example, in the first two cases (a) and (b) we do not expect any intensity from the π band, as it is derived from C $2p$ orbitals that have a node at $q_z=0$. Indeed we observe only one parabola, corresponding to the lowest band σ_1. Along the Γ-M direction [Fig. 2(a)] this band disperses upwards and crosses the first BZ boundary at $q\simeq 0.8$ a.u. In the second BZ the band σ_2 is populated. The minor splitting between σ_1 and σ_2 of $\simeq 1$ eV is not resolved. The band σ_2 continues dispersing upwards until it reaches the maximum at $q\simeq 1.6$ which corresponds to the Γ point in the second BZ. Beyond this point the band turns over. However, the occupation of the band decreases quickly at this momentum value. Hence we do not observe any intensity beyond the maximum.

Case (b) is somewhat more interesting. Along the Γ-K direction [Fig. 2(b)] the σ_1 band disperses up and reaches the BZ boundary at slightly larger momentum ($q\simeq 0.9$ a.u.). Here the population switches from σ_1 to σ_3, as we enter the third BZ. The band gap at K is larger than at M and can be distinguished as a ''kink'' in the measured intensity. Continuing along the same direction in the third BZ the band σ_3 reaches a maximum at the point M at a momentum value of $\simeq 1.3$ a.u. This maximum is observed at a smaller binding energy than the maximum in case (a). Also the momentum density, although decreasing, extends beyond this point, and indeed the band can be seen to turn over on the experimental momentum density plot. The spectrum at the M point we have measured in the Γ-K direction is not equivalent, neither in binding energy nor in intensity, to the spectrum measured at M in the Γ-M direction. This is so because the band σ_3, rather than σ_1,σ_2, is populated. Thus using $(e,2e)$ spectroscopy we can determine the electronic structure in the extended zone scheme.

In case (c) we have a nonzero $q_z=0.41$ a.u. So we expect the π band to be populated. And indeed we observe the two parabolas, one associated with the π band and one with the σ band [Fig. 2(c)]. In this measurement we measure along a line that does not contain zero momentum and hence the measured bottom of the σ band has moved up considerably in energy.

All these effects are nicely reproduced in the theory, shown as well in this figure. We have calculated the momentum space magnitude of the orbitals using a linear muffin-tin orbital (LMTO) model[13] and convoluted this with a 2 eV energy broadening and 0.1 a.u. momentum broadening. This energy broadening is more than the experimental determined width of the C $1s$ level (0.9 eV as determined by this spectrometer and hence the energy resolution of the spectrometer), and mimics the average lifetime broadening of the valence band orbitals as well.

The theoretical plot in Fig. 2 has more contrast than the measurement. This is due to multiple-scattering effects in the

measurement. By this we mean that some of the coincidence events have deflections and/or energy loss associated with them, due to mechanisms other than the $(e,2e)$ event itself. In principle these effects can be simulated quite well by Monte Carlo calculations.[11] Here we present only the raw data since a semiquantitative comparison is straight forward in all cases because there is a clear relation, both in energy dispersion and intensity, between the measurement and the magnitude of the calculated orbitals in momentum space.

In conclusion, it was possible to measure the energy-momentum densities of a single crystal (graphite) with sufficient accuracy to make a detailed comparison with theory. The different crystal directions were clearly distinguished. The node of the π band in the $p_z=0$ plane is clearly identified. These energy-momentum densities resemble closely the magnitude of the orbitals in momentum space. In this way we get a very clear picture of the anisotropic nature of the orbitals in graphite.

This research was funded by a grant of the Australian Research Council.

[1] I.E. McCarthy and E. Weigold, Rep. Prog. Phys. **54**, 789 (1991).
[2] M. Vos and I.E. McCarthy, Rev. Mod. Phys. **67**, 713 (1995).
[3] J.R. Dennison and A.L. Ritter, J. Electron Spectrosc. Relat. Phenom. **77**, 99 (1996).
[4] F. Bell, Th. Tschentscher, J.R. Schneider, and A.J. Rolandson, J. Phys. Condens. Matter **3**, 5587 (1991).
[5] C. Blaas, J. Redinger, S. Manninen, V. Honkimaki, K. Hamalainen, and P. Suortti, Phys. Rev. Lett. **75**, 1984 (1995).
[6] H. Nishimoto, T. Nakatani, T. Matsushita, S. Imada, H. Daimon, and S. Suga, J. Phys. Condens. Matter **8**, 2715 (1996).
[7] A.L. Ritter, J.R. Dennison, and R. Jones, Phys. Rev. Lett. **53**, 2054 (1984).
[8] C. Gao, A.L. Ritter, J.R. Dennison, and N.A.W. Holzwarth, Phys. Rev. B **37**, 3914 (1988).
[9] P. Storer, S.A.C. Clark, R.C. Caprari, M. Vos, and E. Weigold, Rev. Sci. Instrum. **65**, 2214 (1994).
[10] S. Canney, I.E. McCarthy, P. Storer, S. Utteridge, M. Vos, and E. Weigold, J. Electron Spectrosc. Relat. Phenom. **83**, 65 (1997).
[11] M. Vos and M. Bottema, Phys. Rev. B **54**, 5946 (1996).
[12] M. Vos, P. Storer, S. Canney, A.S. Kheifets, I.E. McCarthy, and E. Weigold, Phys. Rev. B **50**, 5635 (1994).
[13] A.S. Kheifets and M. Vos, J. Phys. Condens. Matter **7**, 3895 (1995).